Council on Tall Buildings and Urban Habitat Korea

International Journal of
High-Rise Buildings
www.ctbuh-korea.org/ijhrb/index.php

International Journal of High-Rise Buildings
December 2022, Vol 11, No 4, 265-276
https://doi.org/10.21022/IJHRB.2022.11.4.265

Wind Effects on Tall Buildings with a Porous Double-Skin Façade

Shengyu Tian[1], Cassandra Brigden[2], Caroline Kingsford[2], Gang Hu[1], Robert Ong[2†], and K.C.S. Kwok[2]

[1]*School of Civil and Environmental Engineering, Harbin Institute of Technology, Shenzhen 518055, China*
[2]*School of Civil Engineering, The University of Sydney, Sydney, NSW 2006, Australia*

Abstract Double-Skin Facades (DSF) on tall buildings are becoming increasingly common in urban environments due to their ability to provide architectural merit, passive design, acoustic control and even improved structural efficiency. This study aims to understand the effects of porous DSF on the aerodynamic characteristics of tall buildings using wind tunnel tests. High Frequency Force Balance and pressure tests were performed on the CAARC standard tall building model with a variable porous DSF on the windward face. The introduction of a porous DSF did not adversely affect the overall mean forces and moments experienced by the building, with few differences compared to the standard tall building model. There was also minimal variation between the results for the three porosities tested: 50%, 65% and 80%. The presence of a full-height porous DSF was shown to effectively reduce the mean and fluctuating wind pressure on the side face of the building by about 10%, and a porous DSF over the lower half height of the building was almost as effective. This indicates that the porous DSF could be used to reduce the design load on cladding and fixtures on the side faces of tall buildings, where most damage to facades typically occurs.

Keywords tall building, cladding pressure, double-skin façade, porous facade, wind pressure

[†]Corresponding author:
Robert Ong
E-mail:
robert.harsono.ong@gmail.com

1. Introduction

A Double-Skin Facade (DSF) consists of two distinct planar elements separated by an air corridor, generally ranging between 0.2 m to above 2 m in width (Chan et al. 2009). The original purpose of including DSF in the design of tall buildings is to control solar heat gains and losses within a building (Shameri et al. 2011), reduce the effects of weather on a building and improve acoustic insulation (Ding et al. 2005). However, the potential of the DSF system has been extensively exploited. For example, it can be used as a damper device, reducing wind-induced vibrations without requiring a space-consuming damper system (Azad et al. 2013). An effective design of DSF can reduce the necessity to install dampers that mitigate seismic vibrations (Pipitone et al. 2018). A well-designed DSF system can lead to a more efficient structural system and a reduction in energy use during the building's life cycle. DSF are particularly popular in Northern Europe and Japan but are increasing in numbers in Australia (Marques da Silva & Glória Gomes, 2008). They can range in gap width, depending on design requirements of tall buildings, including the aesthetics, ventilation requirements or depth needed to install shading devices (Sinclair et al. 2009). An example of porous DSF is shown in Figure 1.

Wind affects DSF and causes pressure differences between the internal and external sides of the DSF (Grabe 2002; Zhang et al. 2008). These differences depend on the wind direction and the shape and height of the building (Grabe 2002). Several studies have modelled the flow through the air cavity of DSF systems. Zhang et al. (2008) compared the wind load between internal and external facades in different airflow zones through rigid model wind tunnel tests. It was shown that vortex shedding primarily acts on the external facade, while airflow adhesion and collision cause a compression force on the inner facade. This research examined the effects on the DSF rather than on wind-induced forces of the tall building itself. Hassanli et al. (2017) investigated cavity flow for wind energy harvesting and performed a series of wind tunnel tests and CFD simulations on a DSF with a central opening that modelled air movement through the air cavity. With a normal angle to the DSF, the airflow enters the central opening, stagnates and discharges from the side openings due to flow separation at the leading-edge corner. It was shown that turbulence was dissipated across the cavity and that the flow became more uniform for all four angles of wind incidence tested



Figure 1. An example of building with porous DSF: building of Faculty of Engineering, University of Technology Sydney, Australia.

between 0 and 90 degrees.

For three different multi-storey DSF layouts open at the top and bottom to allow free air movement within the cavity, Da Silva & Gomes (2008) demonstrated a layout-dependent inner wall pressure distribution that was considerably different from an unsheltered building. Lou et al. (2012) studied variations in air corridors with an external strip DSF layout on a tall rectangular building using zone modelling validated against experimental results. Both studies concluded that the internal skin's net pressure depends on the DSF layout, air corridor width and wind incidence angle. Recent research has examined additional structural benefits of DSF in reducing wind-induced forces and vibrations of the building (Hu et al. 2017). Both aeroelastic and pressure tests have been used to evaluate the effect of the distribution of DSF for the induced responses on a CAARC (Commonwealth Advisory Aeronautical Research Council) standard tall building model at a 1:400 length scale (Hu et al. 2017). DSF with vertical openings, particularly a centre opening, significantly diminished crosswind effects without detrimentally affecting the alongwind effects (Hu et al. 2017). The pressure distribution along the side faces of the building was greatly reduced with the presence of a central vertical opening compared to a solid DSF and a building without any DSF system (Hu et al. 2017). The reduction in crosswind response is consistent with studies investigating DSF as vibration absorbers (Azad et al. 2013; Pipitone et al. 2018). Hu et al. (2017) proposed that the reduction in pressure fluctuations on the side faces was due to jet flow from the gap between the windward face and facade, which blew away the separated shear layer from the side face creating a less intense interaction (refer to Figure 2). This is consistent with the findings of Ayed et al. (2015) demonstrated that blowing at the leading edge of the side face of a building could separate the shear layer and form a barrier resulting in a less intense, more coherent flow.

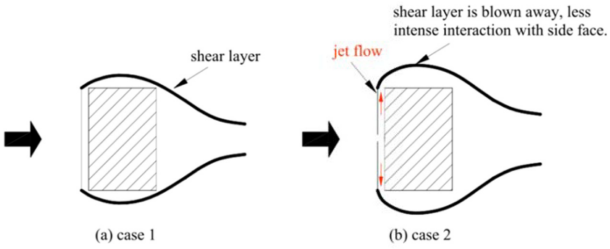


Figure 2. Difference in the airflow on the side face of the building for a building with (a) a solid DSF and (b) a DSF with vertical openings Reproduced from (Hu et al., 2017)

The behaviour of permeable cladding and porous nets can provide insight into the flow behaviour of a porous DSF. The interaction of flow with a porous element causes a pressure drop in the fluid is linked to both mechanical and aerodynamic characteristics of the flow. Effective wind loading on permeable structural elements is a function of the mesh's local velocity pressure and aerodynamic characteristics (Feldmann 2012). It has been shown that local wind loads and net pressures on a permeable element are significantly lower than on an equivalent non-permeable element due to air through-flow (Gerhardt & Kramer 1983; Gerhardt & Janser 1994; Zheng & Zhang 2010; Belloli et al. 2014). Zheng & Zhang (2010) and Belloli et al. (2014) also demonstrated a reduction in the wind-induced dynamic responses, including vortex shedding, vibration and the formation of a wake, for a porous panel compared to an equivalent non-porous panel.

DSF systems, including porous cladding panels and architectural mesh, are becoming increasingly common in modern building practices. Although wind effects on the porous façade have been extensively studied, the effect of the porous DSF on the aerodynamic characteristics of tall buildings remains unknown. This study aims to reveal the effect of the porous DSF on aerodynamic forces and cladding

pressures acting on tall buildings. Both High Frequency Force Balance (HFFB) and pressure tests were performed in the wind tunnel on the CAARC standard tall building model with a variable porous DSF on the windward face.

2. Experimental Setup

2.1. Wind tunnel test configuration and building model

The wind tunnel tests were conducted in the boundary layer wind tunnel at The University of Sydney. The wind tunnel is a closed loop with an inbuilt 250 kW fan and contraction ratio into the test section of 4.5:1. The test section is 2.5 m × 2 m × 20 m with a maximum speed of 27 m/s. The tests were carried out under a turbulent flow, which is equivalent to the flow field of Terrain Category 2 in AS/NZS wind code (AS/NZS 1170.2:2011) and were configured using passive devices to simulate the boundary layer and ensure the model and wind were at approximately the same scale. The mean velocity and turbulence intensity profiles generally agreed with those in AS/NZS 1170.2 for Terrain Category 2, as shown in Figure 3.

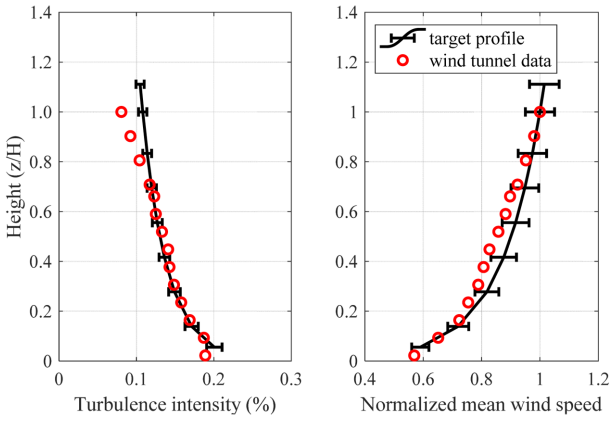


Figure 3. Turbulent intensity and mean wind speed profiles used in wind tunnel tests. A 5% error bar is given.

The HFFB and pressure test models were fabricated using CAARC standard tall building dimensions at 1:200 scale. The HFFB model was constructed from high-density foam and mounted on a high frequency force balance (HFFB) base plate. The pressure testing model was fabricated from 10 mm thick perspex elements with a smooth finish shown in Figure 4. The model was instrumented with 240 pressure taps. The pressure taps were distributed across 10 levels, with 8 taps per level on the windward face, 6 taps per level on the leeward face, and 5 taps per level on the side faces.

2.2. Porous double-skin facades and their pressure loss coefficients

Tests were carried out with a variable DSF mounted on the windward face of both models. The porous DSF elements were modelled with three different porosities: 50%, 65% and 80%. The perforation pattern of the porous facades utilised the same uniform hole pattern with 3 mm diameter holes on an equilateral-triangle pitch. The hole patterns for the three porosities tested are sketched in Figure 5. All these elements were fabricated using a 2 mm laser cut perspex with a smooth finish.

The separation between the inner and outer facades was 5 mm on the model scale, equivalent to 1 m on the real scale. The facade was arranged as a full facade, half facade on the top, or half facade on the bottom of the model for each porosity, as demonstrated in Figure 6. The various configurations were fixed to the model with horizontal 5 mm perspex mounting blocks and double-sided tape to prevent excessive vibration in the wind

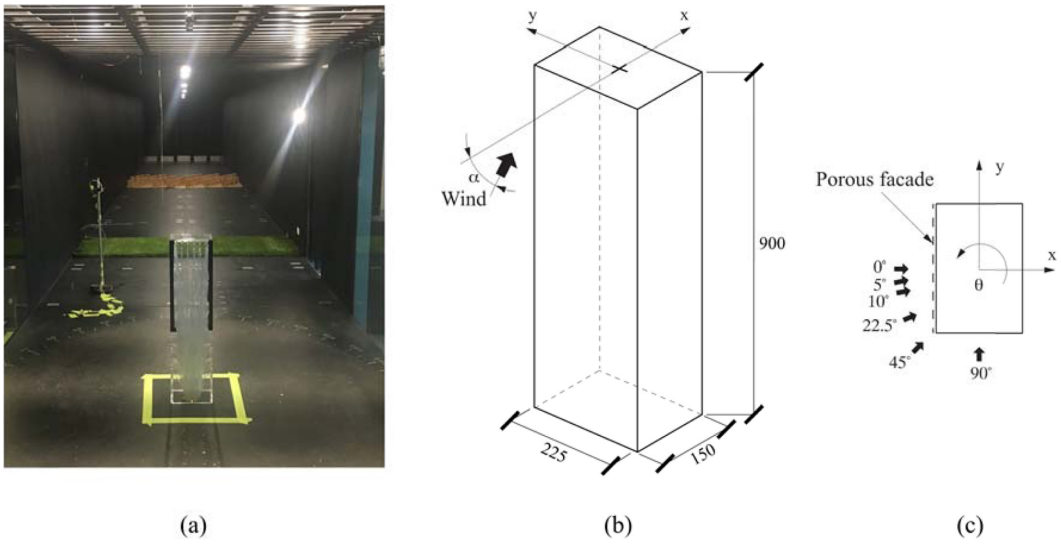


Figure 4. (a) Building model in the wind tunnel, (b) Overall CAARC model dimensions, (c) Angles of wind incidence. All measurements are in millimetres.

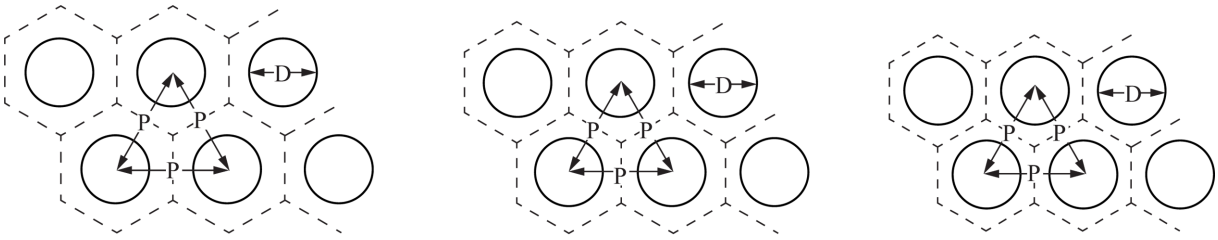


Figure 5. Geometry of porous facade panels with different porosity ratios.

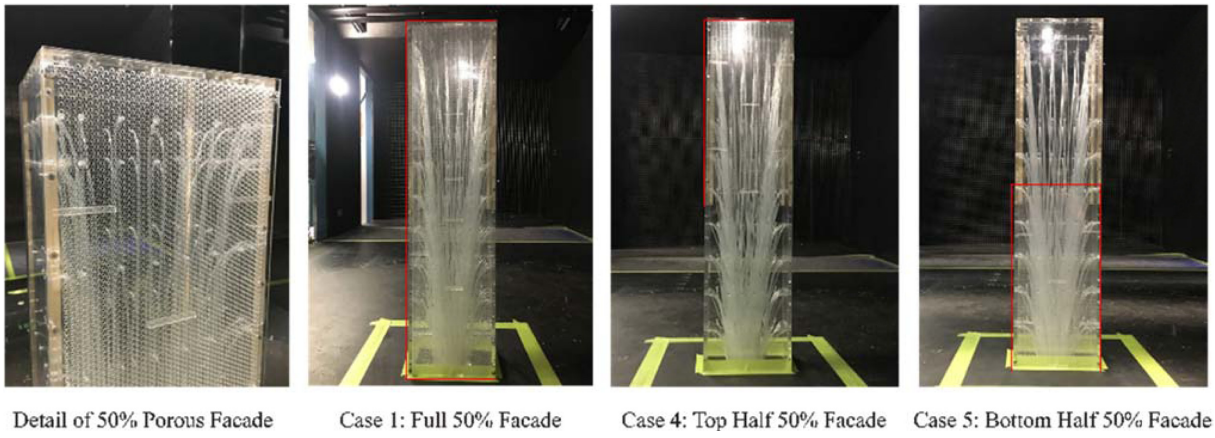


Figure 6. Building model in the wind tunnel fitted with the porous double-skin facade.

tunnel. The blockage ratio inside the wind tunnel due to the model was 4.05%. Six different angles of wind incidence for each facade configuration: 0º, 5º, 10º, 22.5º, 45º and 90º were tested as shown in Figure 4. For both experiments, the reference wind velocity tested was 8 m/s at the top building height with Terrain Category 2 modelled (Australian and New Zealand Standards 2011).

The pressure loss coefficient for each porous facade was measured in preliminary experimental tests in the wind tunnel. Testing was carried out in a timber channel 0.2 m wide × 0.3 m high × 1 m long, as shown in Figure 7. The channel was elevated in the wind tunnel to achieve a more uniform flow compared to a more profiled flow near the ground characteristic of boundary layer flow. Total and static pitot tubes were located at one location upstream and three positions downstream of the facade to measure the pressure loss across the panels. The experiment was repeated twice under the same conditions for 6 wind speeds. The results of the preliminary experiment varied significantly between two repeated trials. The results for the pressure loss coefficient against wind speed is shown in Figure 8. The average pressure loss coefficients for the three DSF with 50%, 65%, and 80% porosities are 5.03, 3.12, and 3.50, respectively.

2.3. Pressure testing and High Frequency Force Balance (HFFB) testing

Pressures acting on the model were collected using pressure sensors. Individual PVC tubing with a 1.6 mm internal diameter connected to 240 pressure taps in the model's surface and two additional tubes measuring total and static pressure, adapted to the pressure sensors using 4 manifolds. A 130PC series piezo-resistive pressure transducer converted the pressure sensed into a voltage. A Halstrup-Walcher Mobile Calibration Device KAL 200 was used to test and calibrate the pressure sensors before each DSF configuration. The sampling duration of each pressure test was 120 seconds. The high frequency force balance measurement system for the experiment was a six axis JR3 2932, with a frequency of 2048 Hz. The duration of each force balance test was 60 seconds.

3. Results and Discussions

3.1. Validation of data

Established data pertaining to the CAARC standard tall building model was compared to data obtained in this experiment for the CAARC model with no facade attached to establish validity. Melbourne (1980) compared the

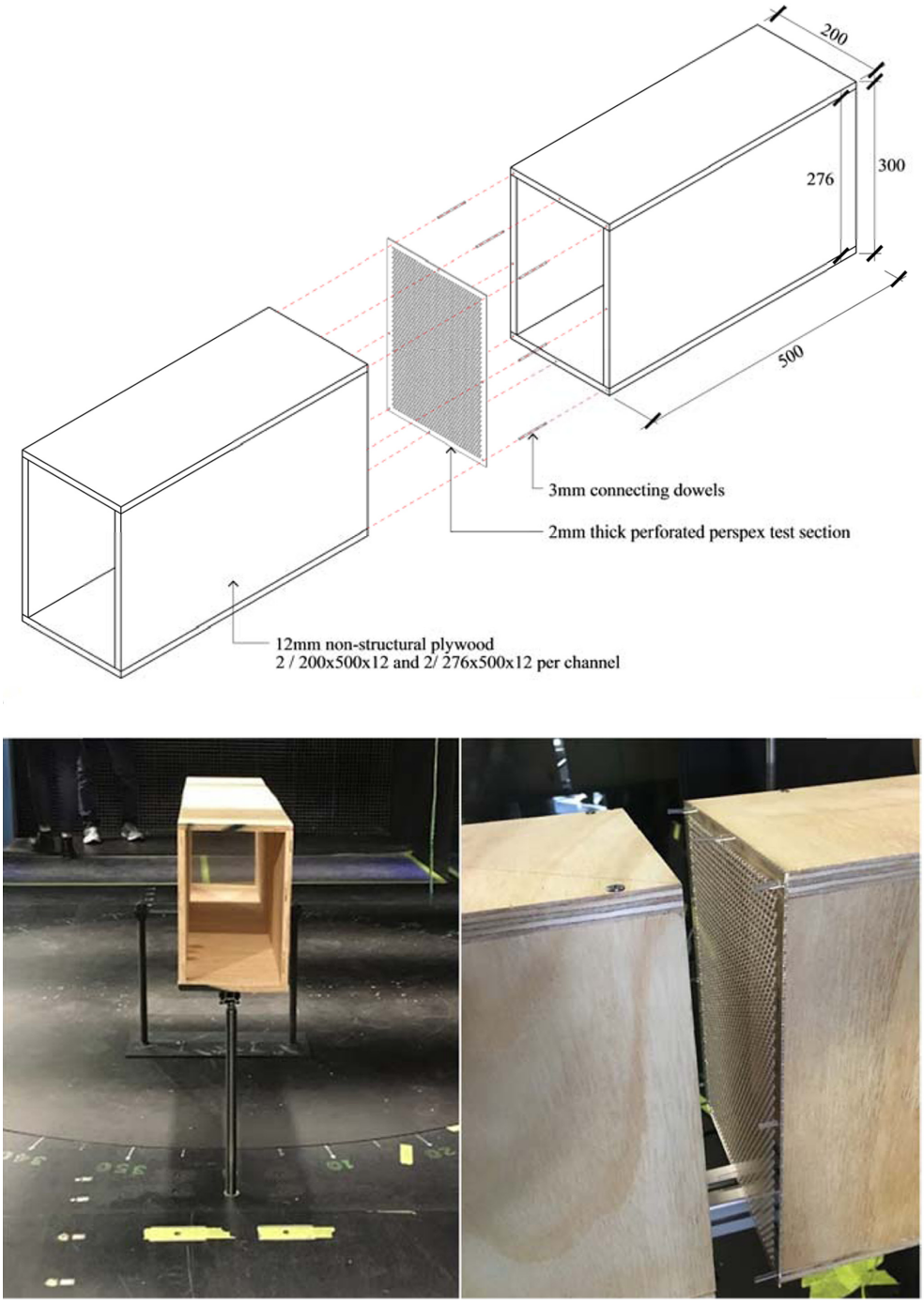


Figure 7. Pressure loss coefficient tests for porous double-skin façades with different porosities in the wind tunnel.

spectral analysis of pressure measurements performed on a CAARC standard tall building by three institutions under various conditions for the same point on each model. An equivalent point was interpolated from the experimental data (no facade attached, zero angle of wind incidence) to enable comparison, shown in Figure 9, which showed good agreement with the published data.

The mean force coefficients from the HFFB test of the CAARC model were also compared to published data from Melbourne (1980) and Obasaju (1992), as shown in Figure 10. In comparing the force coefficients, the experimental results from both tests approximately followed the general trend of the comparison data, shown by a dashed line.

3.2. Pressure distribution on building surfaces

The mean pressure coefficients on the CAARC model at a 0º angle of wind incidence are shown in Figure 11. The windward wall experienced overall positive pressures

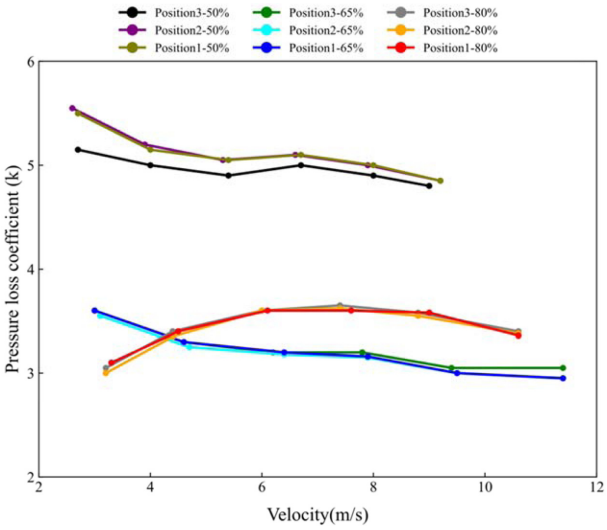


Figure 8. Pressure loss coefficients of porous double skin façade test panels.

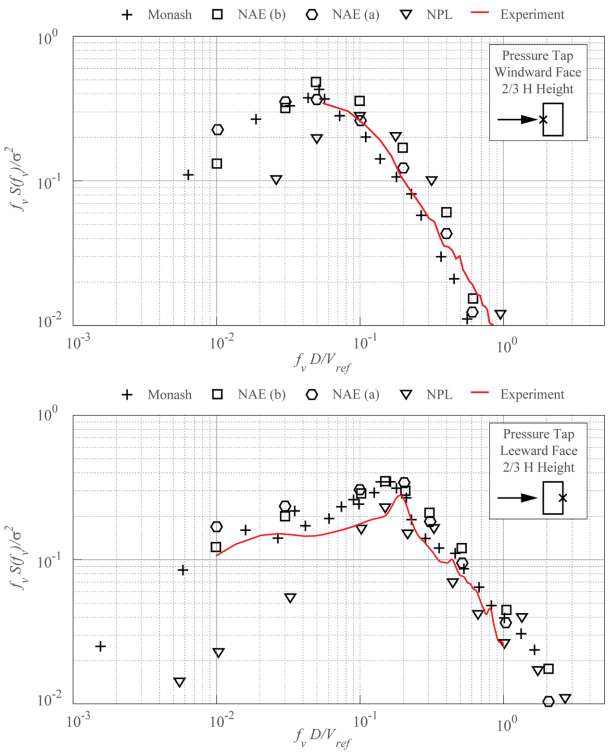


Figure 9. Comparison of spectral analyses of pressure coefficients of windward and leeward sides, centre at 2/3H, of the CAARC model at 0º angle of wind incidence (comparison data from Melbourne, 1980).

with a maximum coefficient of 0.9 corresponding to the stagnation region. The flow split up at the windward face and moved horizontally and vertically around the sharp edges of the building, and exhibited negative pressures on the remaining sides. The distribution of pressure between the two side faces is symmetrical with respect to the oncoming flow, representative of all test cases, as expected.

Pointwise pressure distributions for the localised mean pressure coefficients (Cp) and their standard deviations (SD) along the side face at the highest, middle and lowest levels are shown in Figure 12 and Figure 13. As shown in Figure 12, the models with full 50%, 65% and 80% porous DSF demonstrated a similar trend, indicating a similar magnitude and distribution of mean pressure. Compared to the CAARC model, the mean Cp at Level

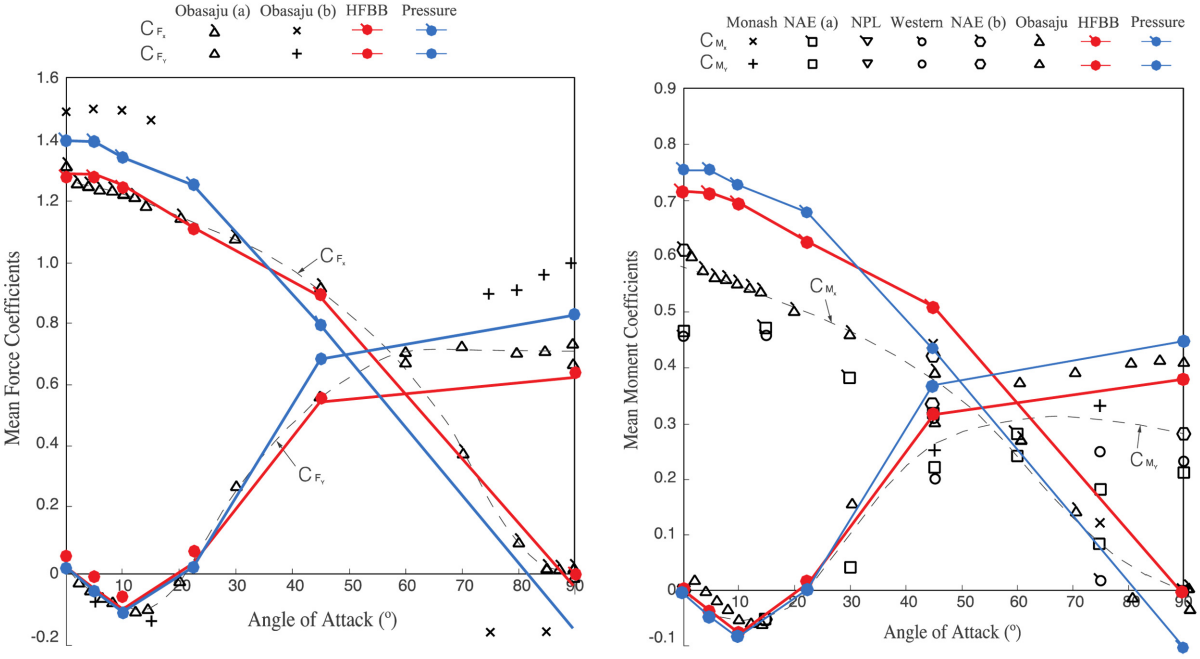


Figure 10. Comparison of mean force and moment coefficients of the CAARC model at 0º angle of wind incidence from HFFB and pressure tests with published data. (comparison data from Melbourne, 1980; Obasaju, 1992).

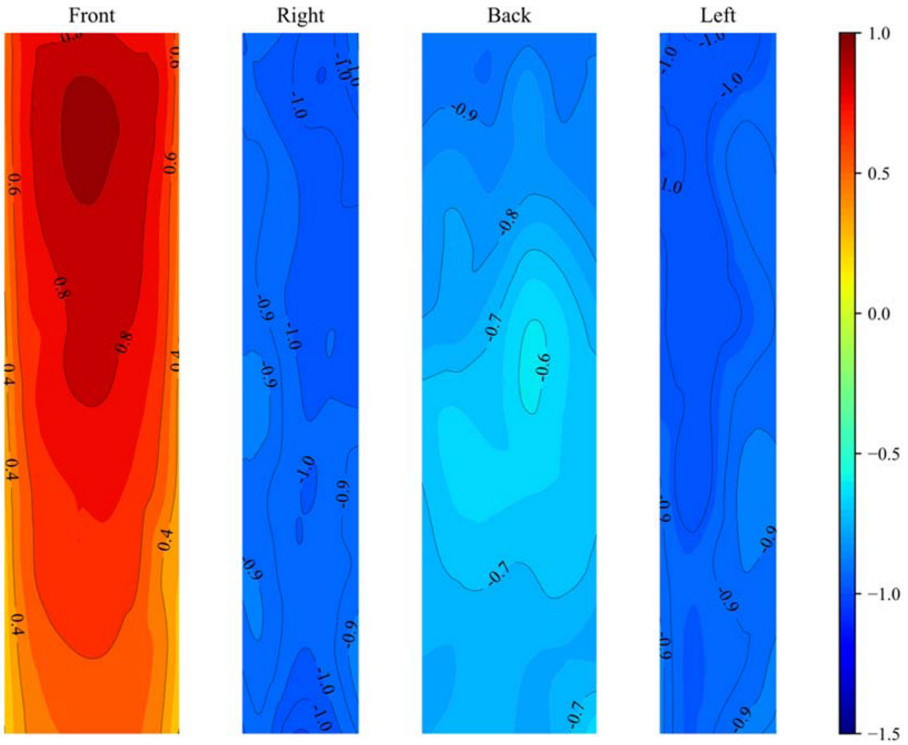


Figure 11. Mean pressure coefficients on the CAARC model with no facade attached for a 0º angle of wind incidence.

1 (the highest level) on the front half part of the side face of the models with porous DSF is significantly less negative, implying the suction is less prominent. In contrast, the mean Cp difference between the models with DSF and the CAARC model on the rear half part of the side face is negligible. At another two levels (Levels 6 and 10), the reduction in the suction is also more significant on the front half part than on the rear half part.

The trend in mean Cp at the highest level (Level 1) for all cases with the porous DSF is reasonably variable from

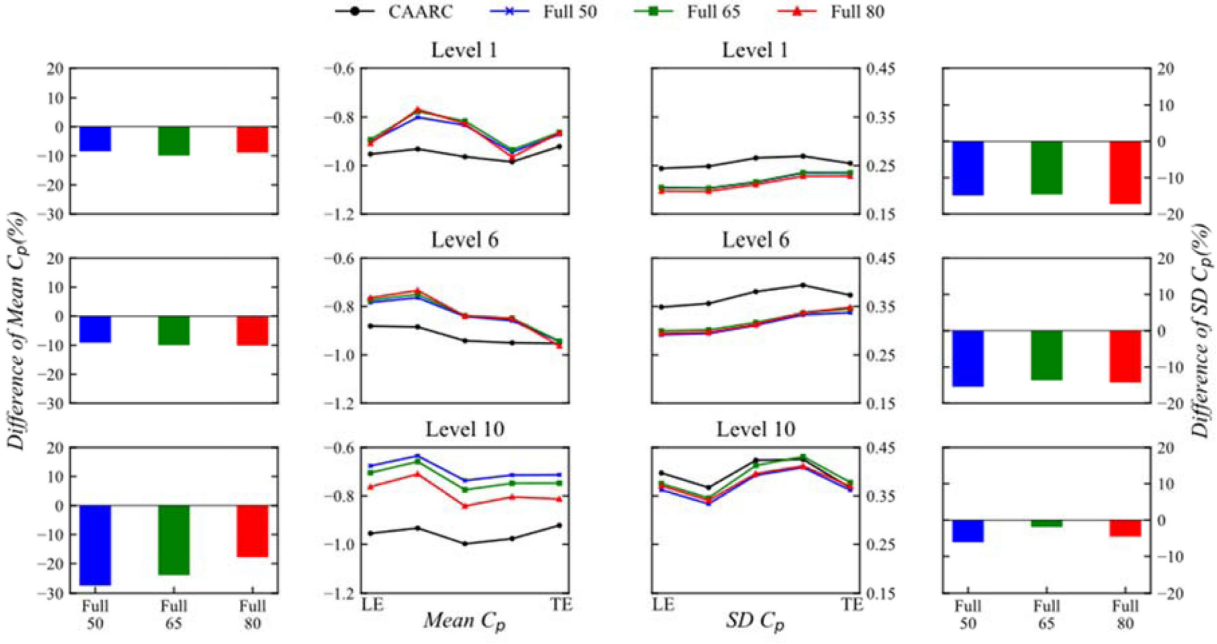


Figure 12. Pointwise pressure and percentage difference on the side face along three rows of the CAARC model, full, 50%, 65% and 80% porous facades at 0º wind incidence. Level 1: the highest level; Level 6: the middle level; Level 10: the lowest level. LE: leading edge; TE: trailing edge.

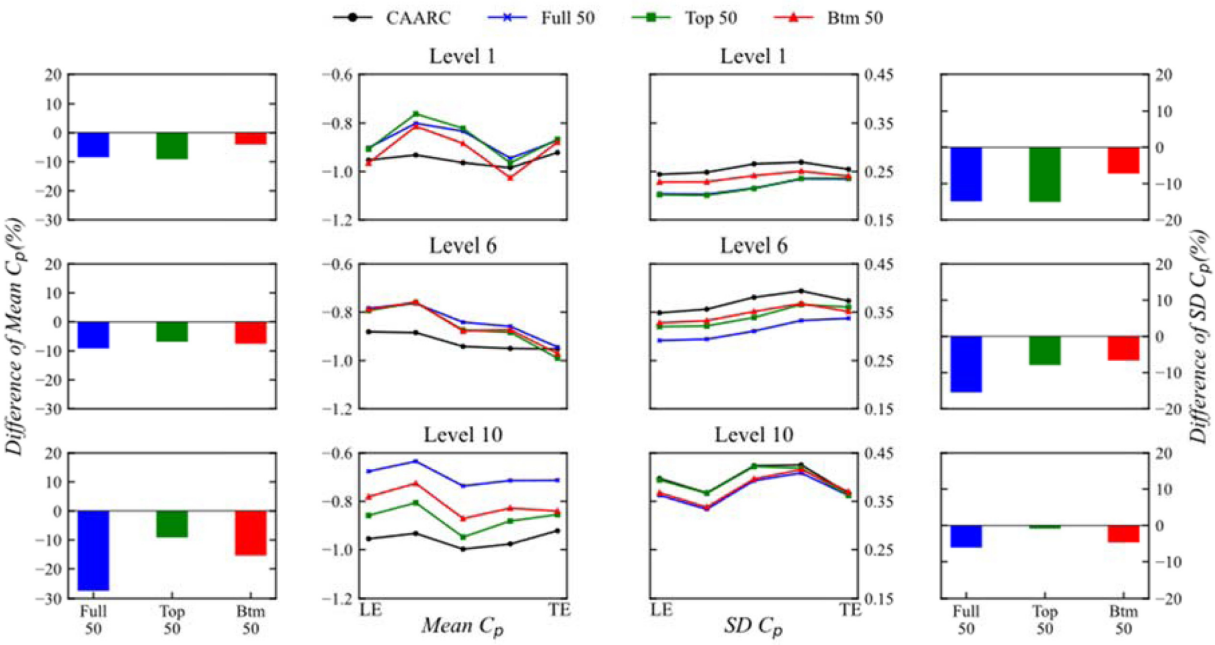


Figure 13. Pointwise pressure and percentage difference on the side face along three rows of the CAARC model, full, top half and bottom half 50% porous facades at 0º wind incidence. LE: leading edge; TE: trailing edge.

leading edge to trailing edge compared to the CAARC model. This may be attributed to the shear layer reattaching to the side face or an increase in curvature of the shear layer shifting the reattachment region slightly upstream (Hu et al. 2016). There is an average decrease in pressure of about 10% across the whole surface for the full porous DSF configurations, with little change between the different porosities. There is also a marked reduction over the bottom half of the building's height of about 10%.

Standard deviation is used to investigate pressure fluctuations on the side faces due to incident turbulence and the unsteady separation zone emanating from the windward edge, associated with vortex shedding, flow separation and reattachment. Both the full facade and bottom half facades generally achieve considerable reductions in pressure fluctuations overall on the side face, as shown in Figure 13 for the 50% porous DSF test case. The top half facade is somewhat effective in reducing the SD of the pressure coefficients in the top and middle regions of the model by 15% and 8%, respectively. However, it is ineffective in reducing the magnitude in the region of maximum pressure fluctuations at the base of the model. This is representative of all the top half porous DSF test cases.

The decrease in pressure and fluctuations on the side face may be attributed to a decrease in mean wind speed after interacting with the porous facades on the windward face. The oncoming flow could be separated into weaker flows as it splits up and moves horizontally and vertically around the building with the presence of the porous DSF. The decrease in pressure fluctuations may also be attributed to air flow discharges outward from the cavity between the DSF and windward wall. Some of the oncoming air flow may be thought to pass through the porous facade, move horizontally outward along the windward face and discharge from the air cavity between the DSF and windward face. This discharge could then blow the separated shear layer and wake region outward at the leading edge, resulting in less interaction with the side face and more coherence in the wake region. This second notion aligns with experimental results and presumptions from Hu et al. (2017) on the wind-induced responses of a building due to a DSF with vertical openings and numerical studies from Ayed et al. (2015) on blowing induced at the leading edge of a prism.

Cladding design is usually governed by peak pressures, a function of the mean pressure and its fluctuation about the mean, acting over a small building region where the external pressures are highly correlated. A porous DSF could be utilised to reduce the peak pressure design load on cladding and fixtures, and they could be used to design more cost-effective cladding systems and improve the overall efficiency in the design of cladding and facades.

3.3. Force and moment coefficients in HFFB testing

The introduction of a porous facade did not affect the overall mean forces and moments experienced by the building (Figure 14-17). This is because, compared to the CAARC model, the models with porous DSF followed the same trend for the force and moment coefficients at different wind attack angles. However, the introduction of the porous facade affected the crosswind fluctuations in some test cases. The 80% porous facade on the windward face of the building aided in reducing crosswind fluctuations

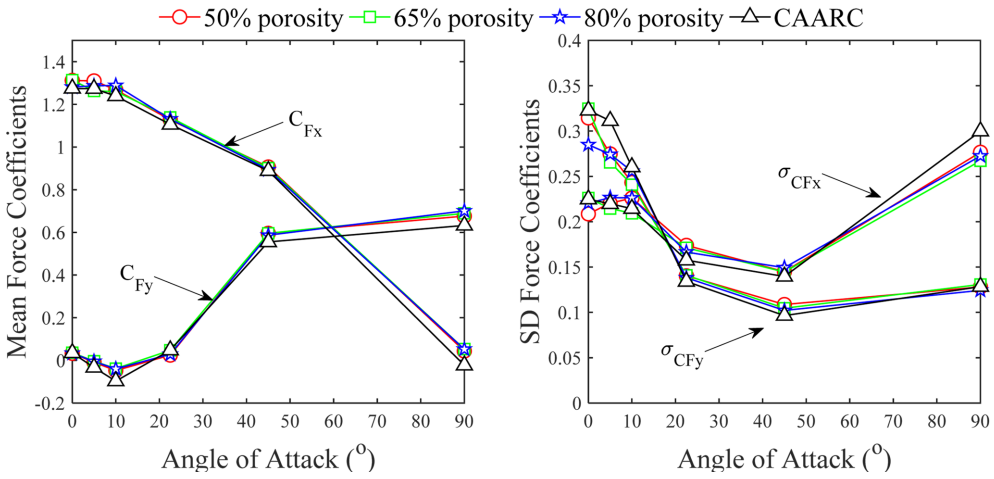


Figure 14. Comparison of mean and standard deviation of force coefficients for the CAARC standard model and the full facade configuration with the three different porosities in relation to different angles of wind attack.

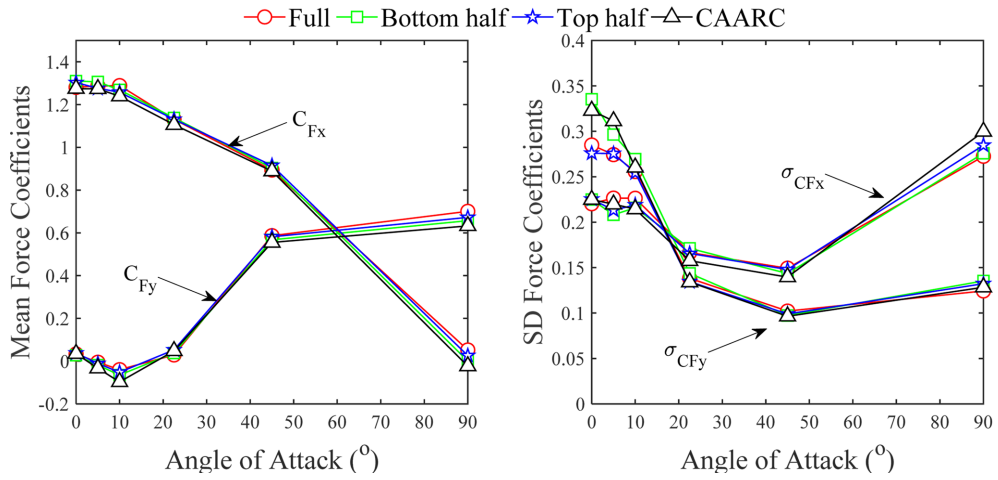


Figure 15. Comparison of mean and standard deviation of force coefficients for the CAARC model and three different configurations with 80% porosity in relation to different angles of wind attack. The configurations tested were the full facade, bottom half facade and top half facade.

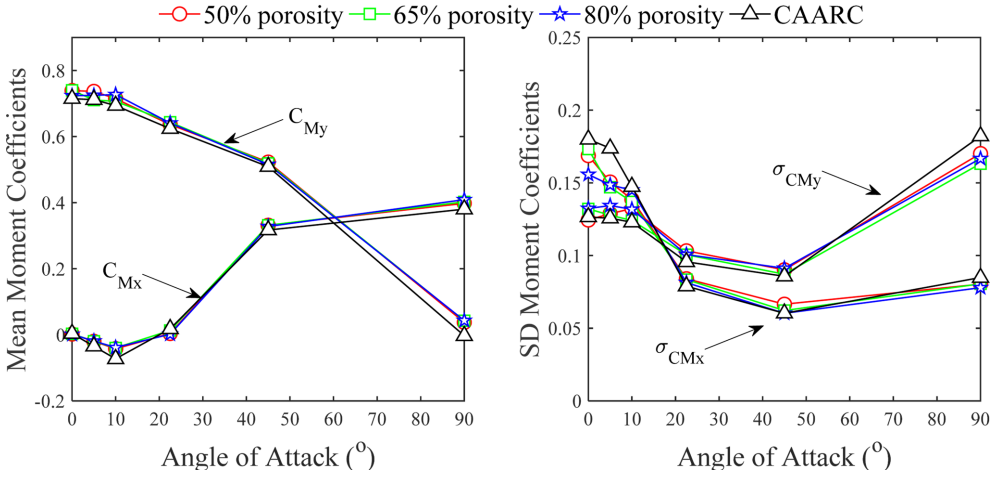


Figure 16. Comparison of mean and standard deviation of moment coefficients for the CAARC standard model and the full facade configuration with the three different porosities in relation to different angles of wind attack.

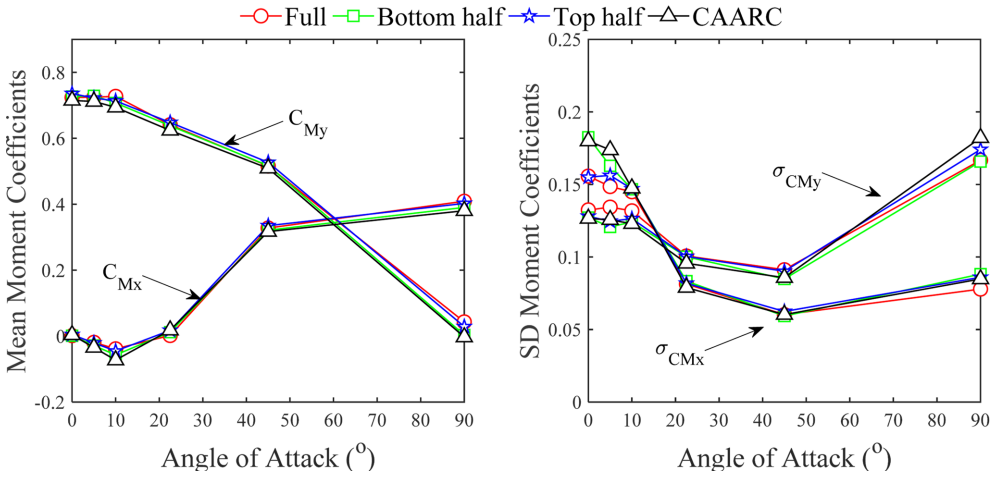


Figure 17. Comparison of mean and standard deviation of moment coefficients for the CAARC model and three different configurations with 80% porosity in relation to different angles of wind attack. The configurations tested were the full facade, bottom half facade and top half facade.

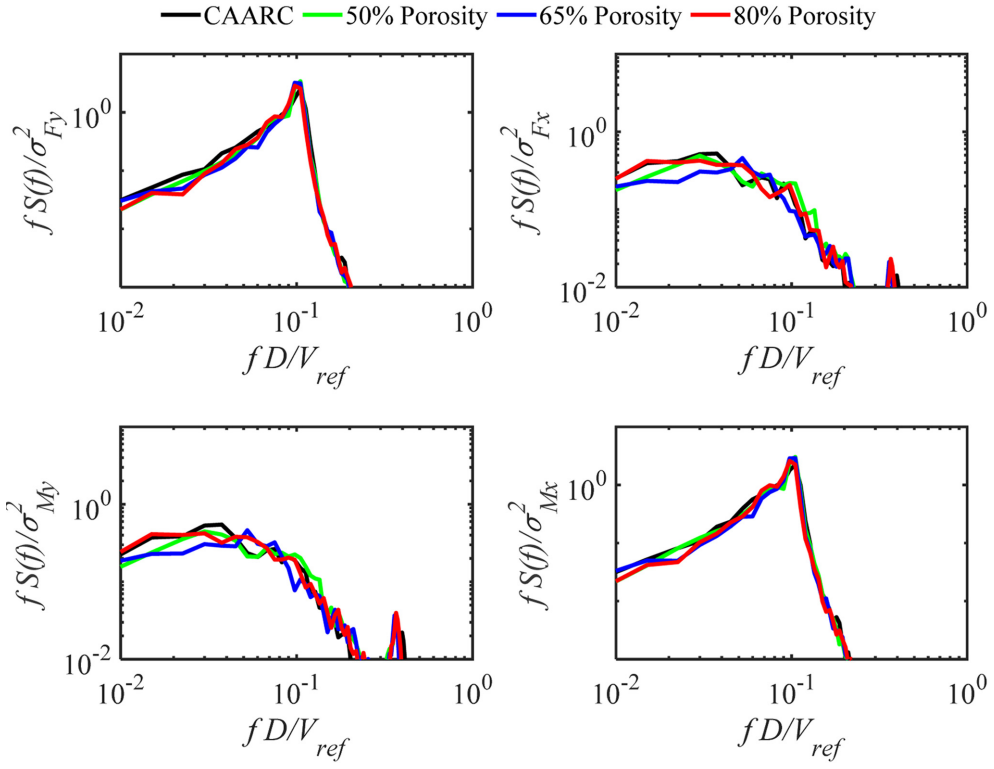


Figure 18. Spectral analysis graphs for Fx, Fy, Mx, and My frequency components, comparing the CAARC model and three test cases of different full facade porosities at 0° wind attack angle.

at 0°, thereby allowing the shear layer to reattach sooner to the building side face (Figure 14 & 16). This could be due to the jet flow effect of the wind as it escaped from the gap between the porous facade and the building face. This aligned with previous research, which suggested that this jet flow formed a barrier between the shear layer and the side face (Hu et al. 2017). For a non-porous facade with a centre opening, the air passed through the opening in the facade and then flowed within the cavity between the facade and the building face (Hu et al. 2017).

Similarly, in this experiment, the air passed through the porous facade and caused a decrease in crosswind fluctuations. The subsequent crosswind fluctuations were weakened by causing these shear layers to reattach sooner along the building side face. The full facade and top half facade of 80% porosity also helped weaken the crosswind

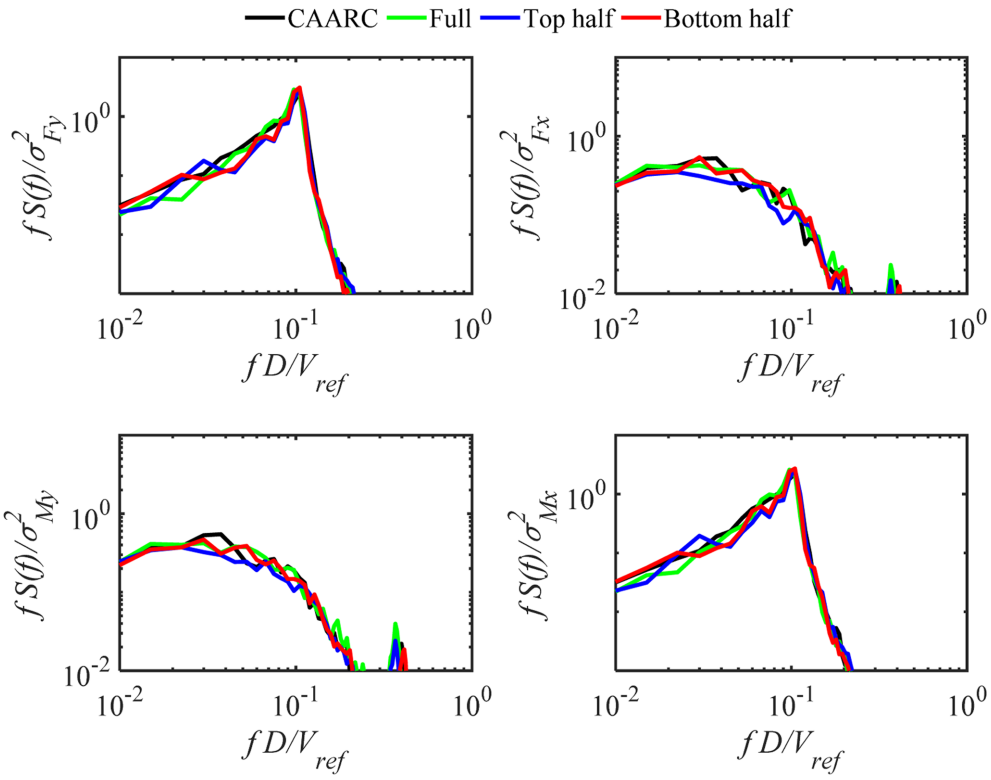


Figure 19. Spectral analysis graphs for Fx, Fy, Mx, and My frequency components, comparing the CAARC model and three 80% porous test case configurations at 0° wind attack angle.

fluctuations at 0° (Figure 15 & 17). This indicated that a full or top half porous facade on the windward face could help diminish crosswind fluctuations.

3.4. Spectral analyses of generalized forces

The addition of a porous DSF did not affect the vortex shedding frequency of the force when compared to the standard CAARC building. There were no changes in vortex shedding frequency among the test cases of three porosities or the test cases of three different facade configurations (Figure 18 & 19).

4. Conclusions

This study investigated the wind effects on tall buildings due to uniformly porous DSF through pressure and HFFB testing. The overall mean pressure coefficients increase slightly over the side face of a building, most prominently for the full facade configuration. A porous DSF is also associated with a significant decrease in the overall magnitude of pressure fluctuations on the side face of the building, particularly for the full and bottom half facade configurations. This indicated that porous DSF could be used to reduce the cladding design loads on the side faces of tall buildings, where most damage to facades typically occurs. There was little change in the wind flow behaviour between the three different porosities tested, 50%, 65% and 80%, for the same facade configurations.

The results suggested that, when designing a tall building with a porous DSF, there are no changes in the overall crosswind and alongwind forces and moments experienced by the building. Consequently, no concessions are needed to accommodate the additional component in terms of overall forces and moments. However, the slight decrease in crosswind standard deviations for the buildings with certain test cases suggested that the fluctuations in the forces and moments in this direction were lessened. Hence, by including a porous DSF in the design of tall buildings, crosswind fluctuations due to vortex shedding may be reduced. Analysis of the results suggested that the introduction of the porous facade did not alter the frequency of vortex shedding compared to the CAARC model.

References

Ayed, S. B., Ragab, S. A., & Haji, M. R. (2016). Flow control of extreme pressure loads associated with flow separation. Journal of Engineering Mechanics, 142, 04015068.

Azad, A, Samali, B, Ngo, T & Nguyen, C 2013, 'Dynamic behaviour of flexible facade systems in tall buildings subjected to wind loads', in Samali, B, Attard, MM & Song, C (eds.), From Materials to Structures: Advancement through Innovation, CRC Press, United Kingdom.

Belloli, M, Rosa, L & Zasso, A 2014, 'Wind loads and vortex shedding analysis on the effects of the porosity on a high slender tower', Journal of Wind Engineering and

Industrial Aerodynamics, vol. 126, pp. 75-86.
Chan, ALS, Chow, TT, Fong, KF & Lin, Z 2009, 'Investigation on energy performance of double skin façade in Hong Kong', Energy and Buildings, vol. 41, no. 11, pp. 1135-1142.
Cook, N. J. (1982). Calibration of the quasi-static and peak-factor approaches to the assessment of wind loads against the method of Cook and Mayne. Journal of Wind Engineering and Industrial Aerodynamics, 10(3), 315–341. https://doi.org/10.1016/0167-6105(82)90005
Davenport, A. G. (2007). Wind Tunnel Testing: A General Outline. The University of Western Ontario, Faculty of Engineering Science. London, Ontario, Canada.
Ding, W, Hasemi, Y & Yamada, T 2005, 'Natural ventilation performance of a double-skin facade with a solar chimney', Energy and Buildings, vol. 37, pp. 411-418.
Feldmann, FKM 2012, 'Wind Loads for Permeable Cladding Elements with High Porosity', The 2012 World Congress on Advances in Civil, Environmental, and Materials Research, Seoul, Korea.
Gerhardt, HJ & Janser, F 1994, 'Wind loads on wind permeable facades', Journal of Wind Engineering and Industrial Aerodynamics, vol. 53, no. 1, pp. 37-48.
Grabe, JV 2002, 'A prediction tool for the temperature field of double facades', Energy and Buildings, vol. 34, pp. 891-899.
Gratia, E., & De Herde, A. (2004). Natural cooling strategies efficiency in an office building with a double-skin façade. Energy and Buildings, 36(11), 1139–1152. https://doi.org/10.1016/j.enbuild. 2004.05.004
Haver & Boecker. (n.d.). Montes Urales 125, Mexico. Retrieved from https://www.weavingarchitecture.com/fileadmin/contents/Referenzen/Montes_Urales_Mexico/PDF/Montes_Urales_Mexico.pdf
Hu, G, Hassanli, S, Kwok, KCS & Tse, KT 2017, 'Wind-induced responses of a tall building with a double-skin façade system', Journal of Wind Engineering and Industrial Aerodynamics, vol. 168, pp. 91-100.
Lou, W, Huang, M, Zhang, M & Lin, N 2012, 'Experimental and zonal modeling for wind pressures on double-skin facades of a tall building', Energy and Buildings, vol. 54, pp. 179-191.
Marques Da Silva, F & Glória Gomes, M 2008, 'Gap inner pressures in multi-storey double skin facades', Energy and Buildings, vol. 40, no. 8, pp. 1553-1559.
Pipitone, G, Barone, G & Palmeri, A 2018, 'Optimal design of double?skin façades as vibration absorbers', Structural Control and Health Monitoring, vol. 25, no. 2, pp. e2086.
Shameri, MA, Alghoul, MA, Sopian, K, Zain, MFM & Elayeb, O 2011, 'Perspectives of double skin façade systems in buildings and energy saving', Renewable and Sustainable Energy Reviews, vol. 15, no. 3, pp. 1468-1475.
Sinclair, R, Phillips, D & Mezhibovski, V 2009, 'Ventilating Façades', ASHRAE Journal, vol. 51, no. 4, pp. 16-27.
Standards Australia, & Standards New Zealand. (2011). Structural design actions. Part 2: Wind actions (AS/NZS 1170.2:2011). Sydney, N.S.W.; Wellington [N.Z.: Jointly published by SAI Global under licence from Standards Australia; Standards New Zealand.
Zhang, M, Lou, W-J & Chen, Y 2008, 'Wind pressure distribution and gust factor on double-skin facades of high-rise building with rectangular shape', Journal of Zheliang Universitym (Engineering Science), vol. 42, pp. 54-59.
Zheng, C & Zhang, Y 2010, 'Numerical investigation of wind-load reduction for a high-rise building by blowing control', J. Build. Struct, vol. 31, no. 2, pp. S176-S181.